To Study the Mechanism of Waterflooding in Sand Rocks Using NMR Techniques

Wang Weimin, Guo Hekun , Liu Wei, Liu Xiongming, Institute of Porous Flow CNPC
and Ye Chaohui, Wuhan Institute of Mathematics and Physics, The Chinese Academy of Science.

Abstract

The use of low field nuclear magnetic resonance (NMR) for characterizing water displacing oil in sandstone is investigated. A new pore size distribution technique which is based on NMR transverse relaxation time (T_2) distribution is developed and demonstrated. Considerable advantages over conventional flooding experiment techniques for characterizing the oil distribution in different sized pores at each injection stage are demonstrated. The recoveries in various pores at different injection stages show that pore size has a profound effect on the incremental rate of recovery.

Introduction

Nuclear Magnetic Resonance is a rapid and nondestructive measurement that can provide various information about the fluid in porous media.[1,2] The pore size sensitivity nature of NMR measurement in cores has encouraged many efforts to estimate the flow properties.[3,4] This paper illustrates the application of low-field NMR to water displacing oil study.

The principle of NMR measurement is based on detecting the magnetization of the proton which is produced when samples that contain oil or water are put in a magnetic field. There are two important parameters to describe the magnetization movement. One is longitudinal relaxation time (T_1) that defines the movement of magnetization in the direction of static magnetic field. The other is transverse relaxation time (T_2) that defines the movement of magnetization in the plane that is perpendicular to the static magnetic field.

The relationship between longitudinal relaxation and pore size results from the strong relaxivity of the core surface. The relaxation time of fluid in a core is much shorter than that of bulk fluid. For a single pore the relaxation time T_1 is:

$$1/T_1 = \rho_1(S/V) + 1/T_{1b} \qquad (1)$$

ρ_1 is the longitudinal surface relaxivity. T_{1b} is the relaxation time constant of the bulk fluid. S/V is the surface-to-volume ratio. Generally, $1/T_{1b}$ is negligible compared to the longitudinal surface relaxivity. Thus T_1 in a single pore is given by:

$$1/T_1 = \rho_1(S/V) \qquad (2)$$

Although T_1 is directly proportional to the pore size, the measurement of T_1 is more time consuming than the measurement of T_2. Hence, we preferentially measure T_2 for precisely tracing a certain flooding stage.

The T_2 relaxation mechanism in cores is much more complicated than T_1. In addition to surface relaxivity that is the same as T_1, T_2 is subjected to the molecular motion in fluid and self-diffusion in inhomogeneous magnetic fields. However, T_2 contains the same petrophysical information as T_1 when the magnetic field strength is low and measurement time (echo time in CPMG sequence) is short [5,6]. T_2 is given by

$$1/T_2 = \rho_2(S/V) \qquad (3)$$

where ρ_2 is transverse relaxivity of fluid in cores.

Sandstone always contains a number of pores with different sizes. The magnetization M(t) measured in NMR equipment is the sum of single pores with their own relaxation time. NMR transverse relaxation data can be expressed as a sum of exponentials:

$$M(t) = \Sigma A_i \exp(-t/T_{2i}) \qquad (4)$$

where T_{2i} is the transverse relaxation time for the pores with characteristic size i and A_i is the volume fraction of these pores. Equation (4) can be inverted into a T_2 relaxation time distribution by fitting and smoothing [7,8].

In flooding experiments, we used deuterium oxide (D_2O) to displace oil. D_2O has no NMR signal in the flooding procedure. Hence, only oil relaxation distribution was detected. Longer T_2 indicates that the corresponding oil exists in larger pores.

In fact, NMR measurement permits pore size to be obtained in the case when the surface relaxivity ρ_2 in equation (3) is known. In this paper, petrography image analysis and mercury injection data were used to determine ρ_2.

Experiments

NMR measurements were conducted in a home made NMR spectrometer with 1175Gauss magnetic field strength that corresponds to 5MHz for proton resonance frequency. The magnet made from permanent-magnet material has a 130 millimeters bore in the horizontal direction. A nonmagnetic core holder made of fiber glass material was put inside the magnet for water flooding experiments. The whole NMR-waterflooding system is shown in Figure 1.

The CPMG NMR pulse sequence is employed for T_2 measurement during the flooding. One thousand and twenty-four echoes were collected in every measurement process. The spin echo time TE was 150μs. Recovery time TR was 3 seconds. The scan time is 8.

Field core plugs 3.8cm in diameter and roughly 6cm in length were obtained from whole diameter drilled cores. The basic petrophysical parameters of the 4 plugs selected were measured after the plugs were cleaned and dried (see Tab.1). All core plugs were tested using the following experiment procedures:

1. Core plugs were first saturated with D_2O brine that has a saltiness of 2500 mg/l after vacuum-pumping for 12 hours.
2. Core plugs were displaced by oil until no D_2O was produced at the outlet. The oil used was simulated oil composed of crude oil (Henan Oilfield ,China) and kerosene with the viscosity of 6mpa.s.The heavy components such as asphaltenes had been moved from the crude oil by centrifuging and filtering.

3. Core plugs were displaced by D_2O. NMR measurements were taken at 0.0PV, 0.1PV, 0.3PV, 1.5PV, and 3.0PV of D_2O injection.
4. Core plugs were cleaned and dried again. Small samples with 2.5cm diameter and length were cut from the 3.8cm diameter plugs to conduct mercury injection. Thin sections were cut from the core plugs as well for petrography image analysis.

Results

Table 1 lists basic petrophysical parameters and conventional flooding results.

Figure 2 shows the comparison of the T_2 relaxation time distribution for core plug No.4 at the irreducible water saturation condition with that of the bulk crude oil/kerosene mixture used in our experiment.The bulk fluid T_2 spectrum is much narrower and the value of T_2 relaxation time is much bigger than that of surface relaxation.Therefore, we think the bulk fluid relaxation is negligible compared to the surface relaxation in our experiment.

Petrography image analysis results are shown in Table 2. The maximum pore radius is about 900μm. The average pore radius is around 40μm. The mercury injection results are shown in Table 3. The maximum throat radius is about 130μm. The average throat radius is around 6μm. Combining these data with NMR T_2 relaxation time distribution (see Fig.4-7), the surface relaxivity ρ_2 can be determined as 0.1μm/s. The pore size distribution from NMR and the throat size distribution from mercury injection for core plug No.4 are shown in Figure 3. The shape of the two curves is similar. However, the difference is increased when the pore size is bigger than 10μm. This results from the fact that the pore size is much bigger than its throat if the pore is big and mercury injection is not an exact method to measure the pore size when the pore is big.

Figure 4 to Figure 7 are the oil distribution for 4 plugs at different water injection stages. We take the core plug No.1 as an example (see Fig.4). Oil distribution in the pores range from 0.5μm to 1000μm at the irreducible water saturation condition, 0.5μm to 850μm at 0.1PV water injection stage, 0.5μm to 580μm at 0.3PV water injection stage, 0.5μm to 520 μm at 1.5PV water injection stage, and 0.5μm to 460μm at 3.0PV water injection stage. Figure 4 shows that only the oil existing in pores that are bigger than 2.58μm can be displaced during the water injected and the oil can not move when it existed in pores that are smaller than 2.58μm. To core plug No.1, we define 2.58μm as the cut off pore size of moveable oil. Oil existing in pores that are smaller than 2.58μm was bounded by capillary pressure and viscous forces and can not be displaced by water. Different samples have different cut off pore sizes(see Tab.4). The moveable oil percentage,which is defined as the ratio of integrated area to the right of the cut off pore size to the total integrated area below the pore size curve, can be calculated. Results are in table 4. The recovery of different sized pores at each injection stage can be calculated as well with the similar way(see Fig.8).

Analyzing Figure 3 to Figure 7, we can find that the oil existing in different pores bigger than cut off pore sizes was displaced by water almost at the same time. But the incremental rates of recovery for various pores differ from each other a lot and change at each stage.

The pores of the core plug No.1 were divided into three groups to illustrate the change of recovery for different sized pores at different injection stages (Fig.8). The oil recovery of big pores increases rapidly in the beginning and comes to a fixed value quickly as water was injected. The oil recovery of medium sized pores increases smoothly during the whole displacement period. The recovery of small pores is very low at the beginning and increases slowly after 0.1PV water injected. The residual oil exists almost in every sized pores but mainly in medium and small pores after water cut is over 90%.

Conclusions

1. Low field magnetic resonance technique has many advantages to investigate water flooding in sandstone.
2. NMR transverse relaxation time T_2 spectra can be scaled into pore size distributions with the aid of petrography image analysis and mercury injection data.
3. Oil existing in pores smaller than the cut off pore size is bounded by capillary pressure and viscous forces and can not be displaced by water. A cut off pore size or T_2 relaxation time can be used to determine the moveable oil percentage in sandstone.
4. The incremental rate of recoveries for different sized pores differs from each other. The big pores come to a fixed recovery value quickly. The recovery of medium sized pores increases smoothly. And the small pores increase slowly in recovery.

References

1. Timur, A.: “Pulsed Nuclear Magnetic Resonance Studies of Porosity, Moveable Fluid, and Permeability of Sandstone,” *JPT* (1969)21, 775-786.
2. Kenyon, W.E.,Day, P.I., Straley, C., and Willemen, J.F.: “Three-Parts Study of NMR Longitudinal Relaxation Studies of Water- Saturated Sandstones,” SPE Formation Evaluation (Sept. 1988) 622-636.
3. Baldwin, B.A., Yamanashi, W.S,: “NMR Imaging of Fluid Dynamics in Reservoir Core,” *Magn. Reson. Imaging* 6:489-500;1988.
4. Howard, J.J., and E.A. Spinler,: “Wettability and Fluid Saturations Determined from NMR T1 Distributions,” *Magn. Reson. Imaging* (1994) 12,197-200.
5. Bergman, D.J., Dunn, K.J.,: “Magnetic Susceptibility Contrasted Fixed Field Gradient Effects on the Spin-Echo Amplitude in a Periodic Porous Media with Diffusion,” (1995) Phys. Soc., 40, 695-702.
6. Kleinberg, R. L., Straley, C., Kenyon, W.E.,: “ Nuclear Magnetic Resonance of Rocks: T1 vs. T2, “ SPE 26470, 68th Annual SPE Technical Conference, Houston, Texas, 3-6, Oct., (1993).
7. Dunn, K.J., Latorraca, G.A.,: “On the Calculation and Interpretation of NMR Relaxation Time Distribution,” SPE28367, 69th Annual SPE Technical Conference, New, Orleans, LA, USA, Sept., (1994).
8. Butler, J.P., and Dawson, S.V., : “Estimating Solution of First Kind Integral Equations with Nonnegative Constraints and Optimal Smoothing,” SIAM J.Number.Anal. 18, 381(1981).

Tab.1 The basic petrophysical parameters of core plugs

Sample No.		1	2	3	4
Porosity (%)		14.8	20.4	16.3	19.1
Permeability($\times 10^{-3}mm^2$)		548.6	457.3	139.5	266.4
Irreducible Water Saturation		0.31	0.36	0.33	0.34
Stage 1	Recovery(%)	12.07	10.96	12.88	11.28
	Water cut (%)	0.0	0.0	0.0	0.0
	Pressure gradient (MPa/m)	0.085	0.109	0.363	0.232
Stage 2	Recovery(%)	32.09	29.19	24.01	26.69
	Water cut(%)	14.5	15.2	7.5	11.9
	Pressure gradient (MPa/m)	0.103	0.142	0.403	0.256
Stage 3	Recovery(%)	39.54	38.73	30.19	36.35
	Water cut(%)	49.2	50.0	53.8	54.1
	Pressure gradient (MPa/m)	0.111	0.157	0.444	0.281
Stage 4	Recovery(%)	49.54	45.0	37.10	42.06
	Water cut(%)	92.8	93.3	95.8	96.2
	Pressure gradient (MPa/m)	0.092	0.13	0.415	0.253

Tab.2 Petrography image analysis data

Sample No / Parameters	1	2	3	4
Maximum Pore Radius(μm)	781.61	919.54	769.54	596.55
Average Radius(μm)	40.92	45.90	38.02	30.48
Sorted Index	0.327	0.337	0.302	0.369
Skewness	0.351	0.372	0.331	0.266
Suface/Volume	0.557	0.562	0.751	0.598

Tab.3 Mercury injection data

Sample No / Parameters	1	2	3	4
Maximum Throat(μm)	129.02	126.79	126.79	129.02
Average Throat	5.91	6.42	6.25	7.08
Sorted Index	3.05	3.28	2.99	3.65
Skewness	1.41	1.45	1.32	1.20
Median Throat(μm)	15.25	12.57	11.64	8.83

Tab.4 Oil distribution at different injection stages and moveable oil values

Pore Size Range (μm) / Status \ Sample No	1	2	3	4
Oil Saturated	0.5-1000	0.2-1000	0.1-1000	0.1-900
First Stage	0.5-850	0.2-850	0.1-850	0.1-700
Second Stage	0.5-580	0.2-600	0.1-750	0.1-400
Third Stage	0.5-520	0.2-450	0.1-650	0.1-300
Fourth Stage	0.5-460	0.2-350	0.1-580	0.1-250
Part of moveable Oil	2.58	2.02	2.02	1.58
moveable Oil Percentage(%)	94.1	94.8	93.6	89.9

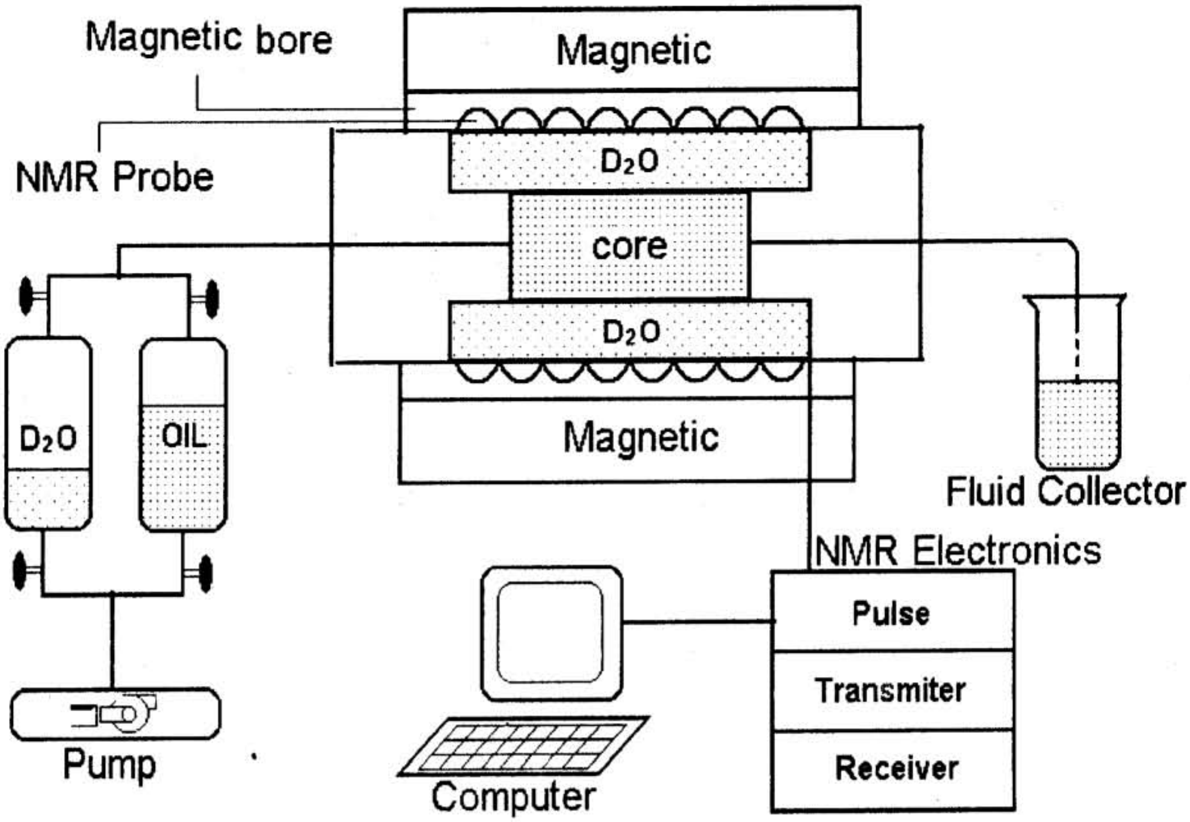

Fig.1 The sketch map of NMR Waterflooding System

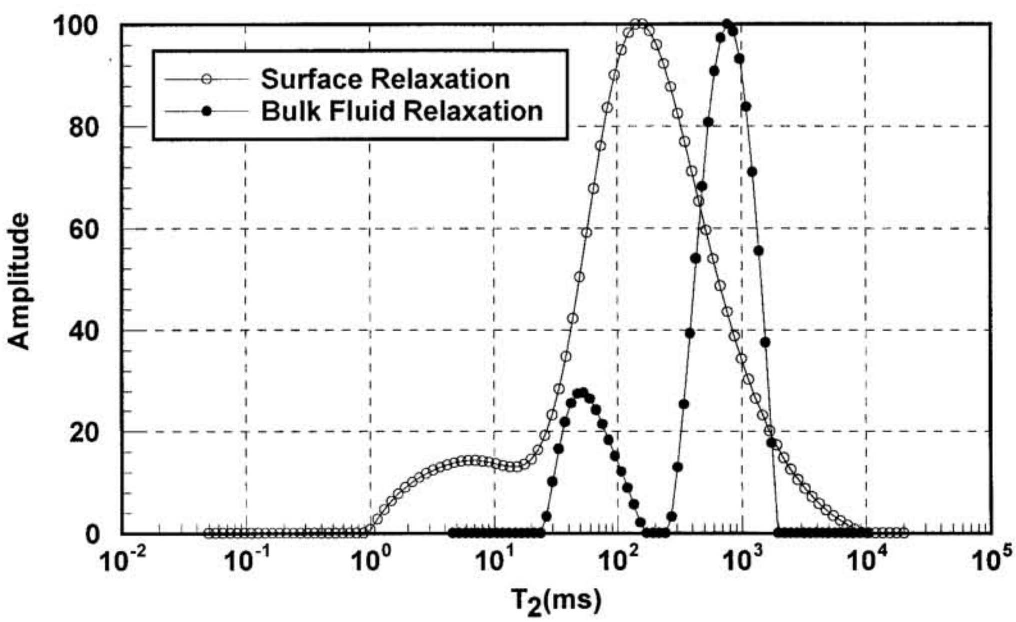

Fig.2 Comparison of bulk fluid relaxation and surface relaxation for core plug No.4

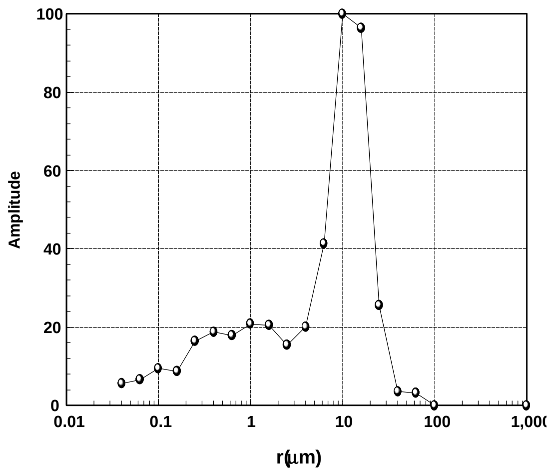

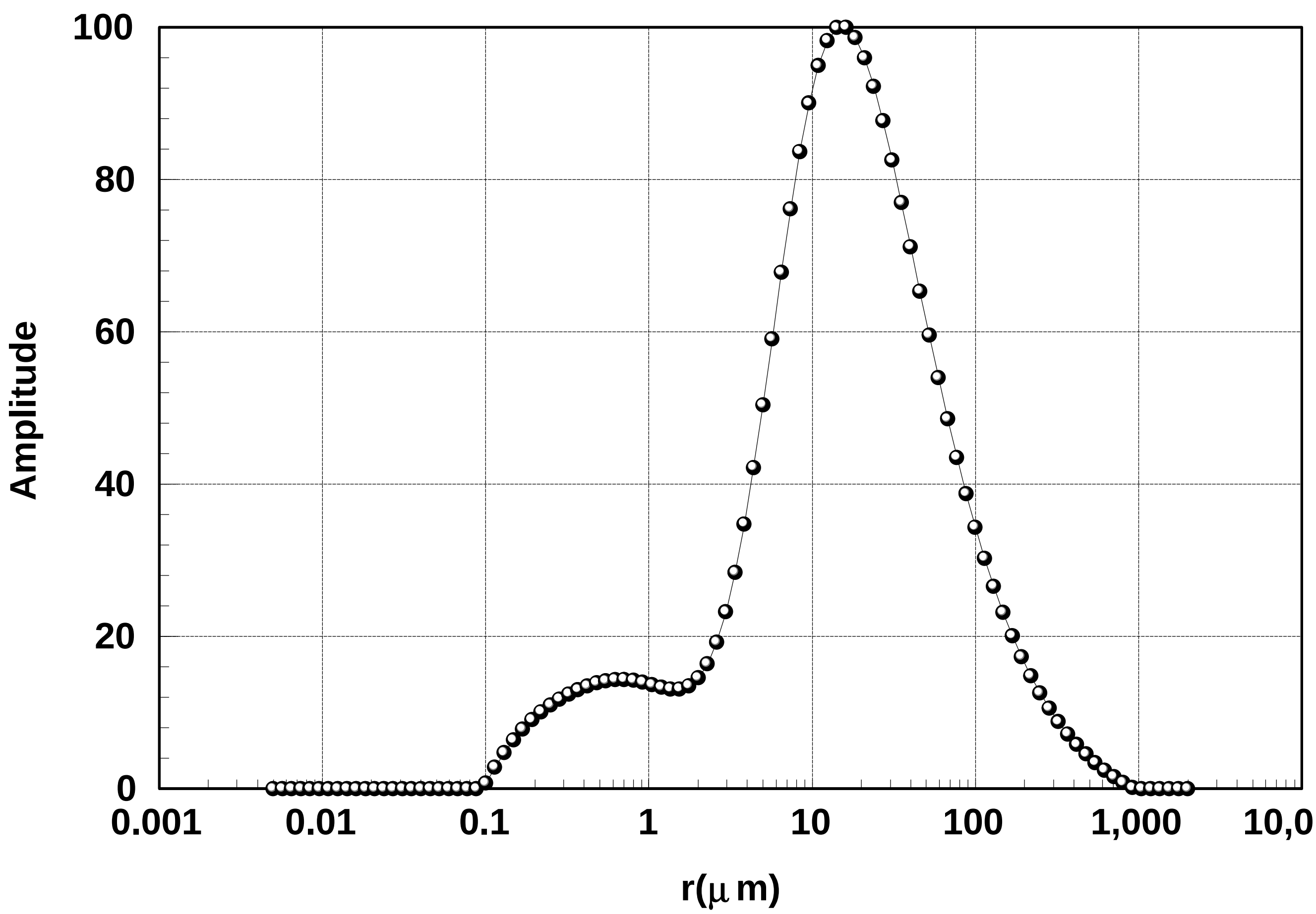

Mercury injection throat size distribution NMR pore size distribution

Fig.3 Distribution of NMR pore size and mercury injection throat size for core plug No.4

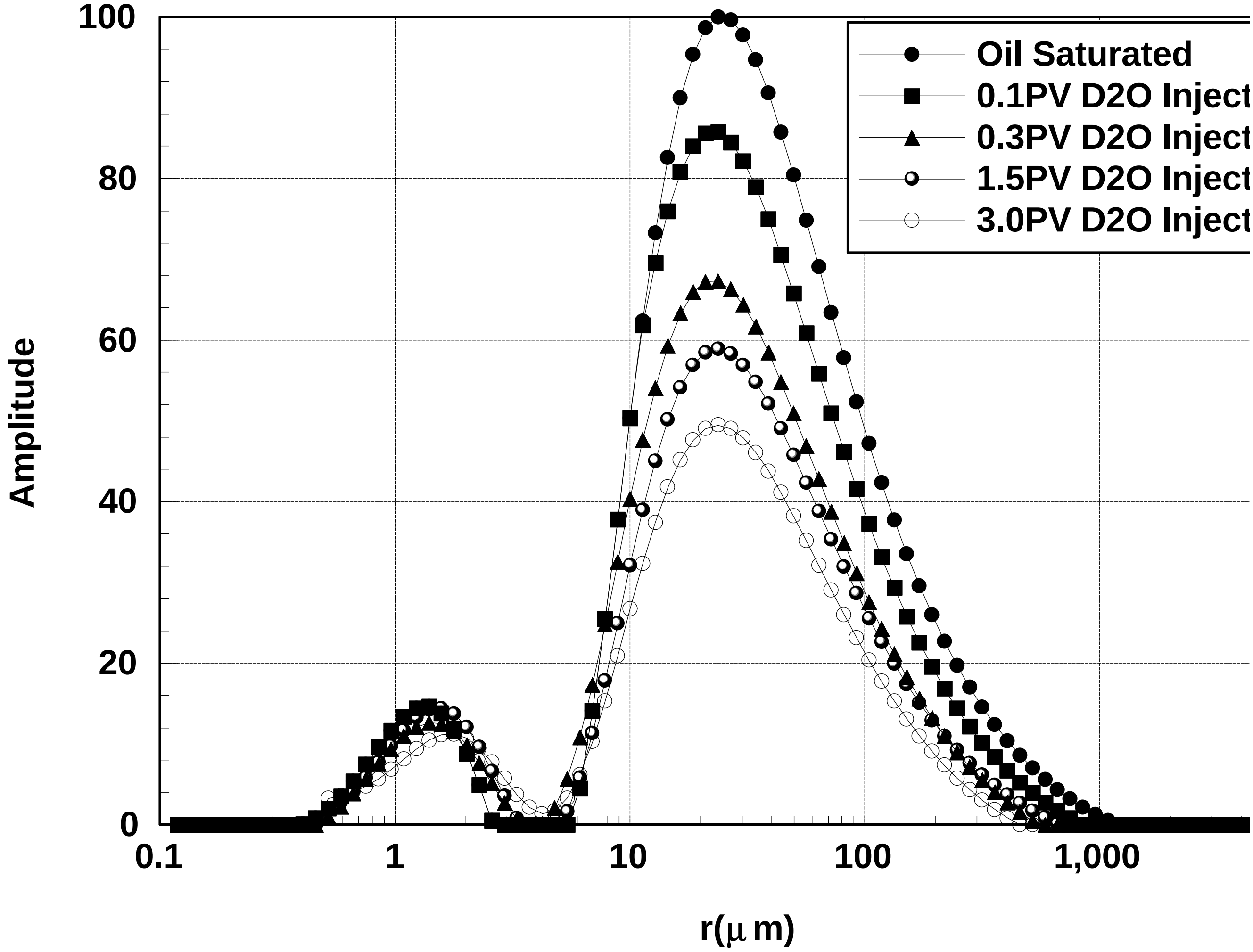

Fig.4 Oil distribution of core plug No.1 at different water injection stages

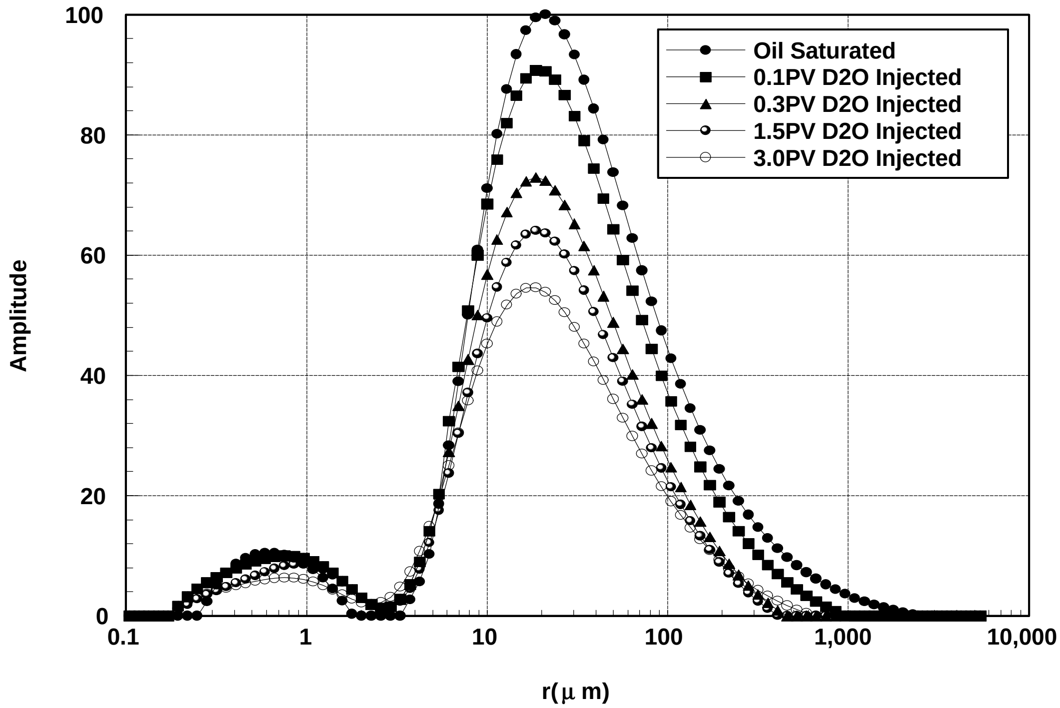

Fig.5 Oil distribution of core plug No.2 at different water injection stages

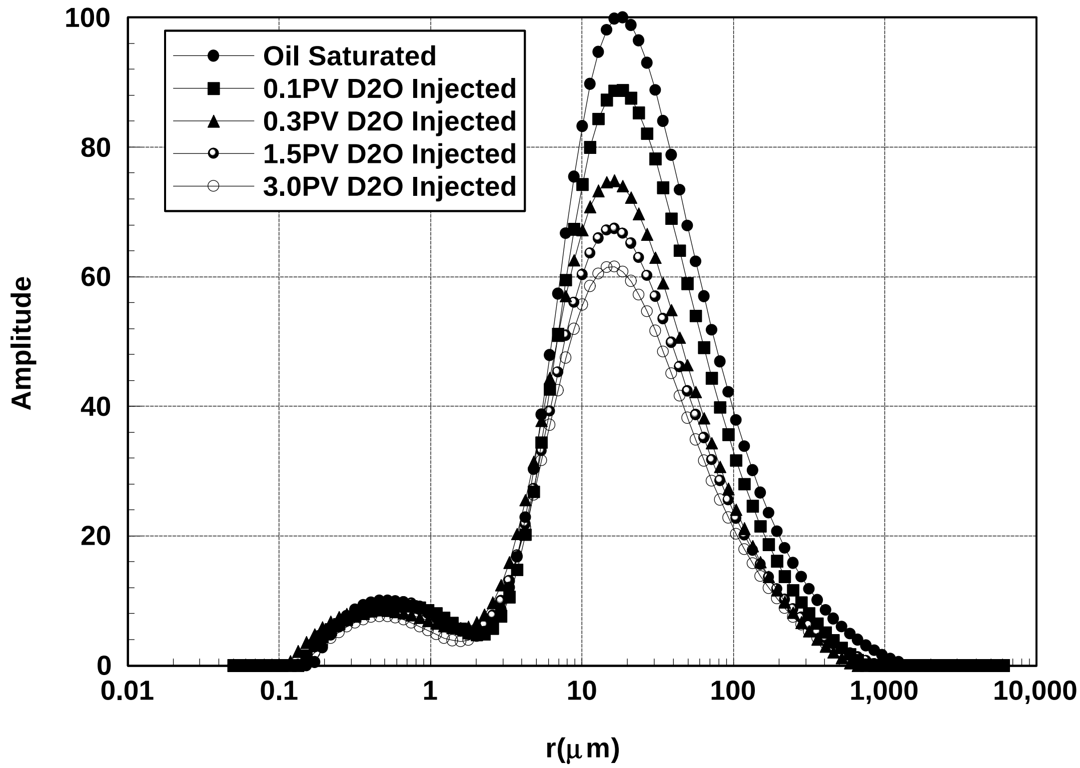

Fig.6 Oil distribution of core plug No.3 at different water injection stages

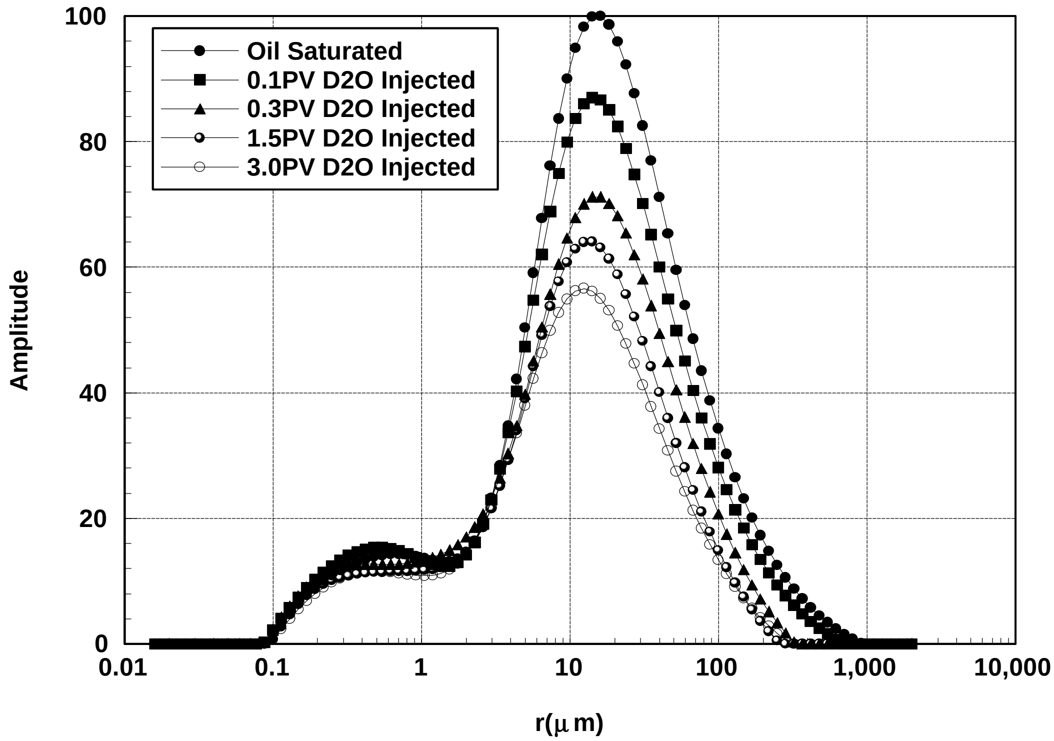

Fig.7 Oil distribution of core plug No.4 at different water injection stages

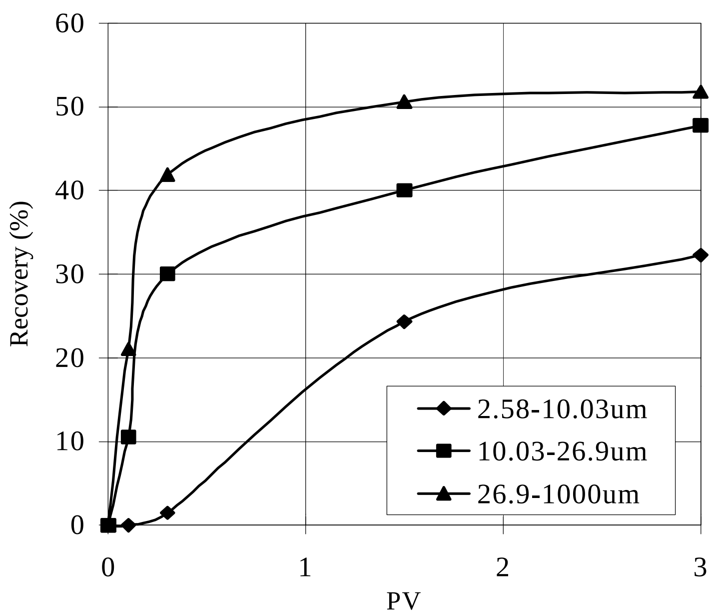

Fig.8 Oil recovery of different sized pores in core plug No.1 at different water injection stages